Ideal Molecular Sieving with a Dense MOF for Helium Upgrading with Highly Diffusion Selective Mixed Matrix Membranes

*Ayisha Komal[1,†], Laura Calderón -Rodríguez[2,†], Oksana Smirnova[1], Eren Grossmann[1], Aparna Binu Varghese[1], Karen Marlenne Garcia Alvarez[3], Andreas Schneemann[3], Thomas Hoyer[4], Ralf Wyrwa[4], Felix Helmut Schacher[2,5,6] and Alexander Knebel[1,5]**

[1] Otto Schott Institute of Materials Research, Friedrich Schiller University of Jena, Center for Energy and Environmental Chemistry II, Lessingstraße 12-14, 07743 Jena, Germany

[2] Institute of Organic Chemistry and Macromolecular Chemistry (IOMC), Friedrich-Schiller-University Jena, Humboldtstraße 10, 07743 Jena, Germany

[3] Technical University Dresden, Chair of Inorganic Chemistry I, Bergstraße 66, 01069 Dresden, Germany

[4] Fraunhofer Institute for Ceramic Technologies and Systems, Michael-Faraday-Straße 1, 07629 Hermsdorf, Germany

[5]Center for Energy and Environmental Chemistry, Friedrich Schiller University Jena, Philosophenweg 7a, 07743 Jena, Germany

[6] Helmholtz Institute for Polymers in Energy Applications Jena (HIPOLE Jena), Lessingstraße 12-14, 07743 Jena, Germany

†These authors contributed equally.

***Corresponding author:** Alexander Knebel, alexander.knebel@uni-jena.de

Keywords: Metal-Organic Frameworks, Gas Separation Membranes, Mixed Matrix Membranes, Helium Upgrading, High Precision Molecular Sieving, Natural Gas Separation, Composite Membranes

Abstract

Helium is one of the most critical resources of our planet, as it is a finite resource, cannot be produced from radioactive decay in sufficient amounts and escapes our atmosphere, while being extraordinarily important for high tech applications in research and medicine. We demonstrate a concept of using the "dense" metal-organic framework (MOF) MIL-116(Ga) as a molecular sieve specifically allowing diffusion of He. Incorporating up to 20 wt.% MIL-116(Ga) into polysulfone, a chemically stable, mechanically robust, and commercially available polymer, high performance mixed matrix membranes were fabricated and tested in gas permeation. The membranes reach He permeabilities up to 37.4 Barrer and He/CH_4 selectivity of 1190, mimicking process conditions with He concentration of 4 % in CH_4. With increasing filler content, permeability of He increases, while CH_4 permeability decreases. Microstructural analysis of the MIL-116(Ga) reveals that the crystals grew into druse-like hollow crystals, highly beneficial for fast He permeability. CH_4, N_2 and CO_2 cannot enter the crystal, as proven by sorption experiments, providing high diffusional selectivity. Furthermore, polymer filler interactions are investigated by scanning electron microscopy and energy dispersive x-ray spectroscopy. We benchmarked the performance to existing composites and polymers, where MIL-116(Ga)-formate stands out with extraordinary membrane performance.

Table of Contents Graphic

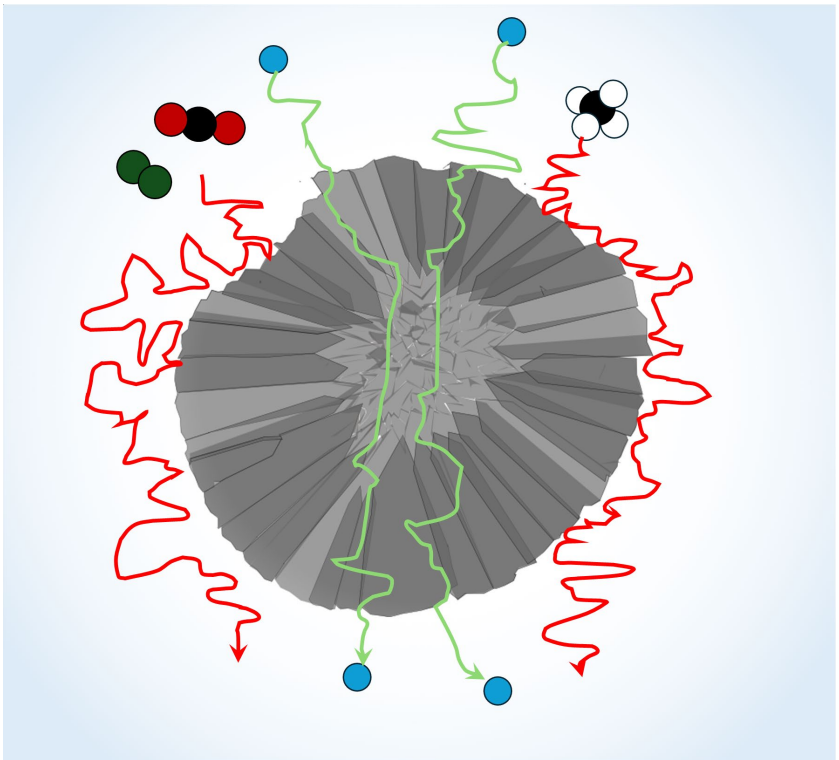

Introduction

The noble gas Helium (He) is the smallest gas (kinetic diameter d_{kin}(He) = 2.60 Å) and is a rare resource, making efficient production important. He is holding significant value for the future of the energy sector and for advancement of different high tech sectors, such as medicine and research.[1] Natural gas (methane, CH_4, d_{kin} = 3.8 Å) as one of the primary fossil energy source can contain up to 4 % He, but usually lower concentrations are observed. The massive fossil fuel exploitation over the past century resulted in highly elevated levels of He in the atmosphere,[2] while there is an ever craving need in the technology sector for He,[3] for example in medical applications, such as MRI (magnet resonance imaging),[4] or technological application in lasers, spectroscopy and deep cooling.[5] Crude He sources are uncommon and have largely ceased exploitation due to their importance for the future of technology.[6] He is a non-renewable resource, thus generating strong interest in its separation from He-rich natural gas.[2] While the components of He-rich natural gas can be separated through cryogenic distillation, an energy efficient process can be developed from diffusion driven molecular sieving membrane technology.[7]

Highly promising molecular sieving materials are Metal-Organic Frameworks (MOFs), hybrid materials consisting of inorganic metal-centres or clusters and organic linker molecules, which are connected via coordination bonds showcasing an extensive array of crystalline structures with a broad spreading from non-porous to highly porous networks.[8] He is usually referred to as a non-adsorptive gas because it requires highly elevated pressure or very low temperatures to show condensation in pore systems, which is why diffusive separation is highly favoured instead.[9] However, discussions have persisted regarding the molecular sieving capabilities of MOFs over recent years.[10] This debate stems from the characteristics of the building blocks — the inorganic metal centre or cluster and the organic linker — as well as the nature of their coordination bonds.[11] While the building blocks offer numerous interesting features, they often render the frameworks unreliable for precise molecular sieving.[12] This unreliability is primarily attributed to the flexibility of the organic components and the linkers, which can undergo rotational conformation changes and show thermal lattice vibrations,[13] along with energetic host-guest interactions contributing to the so-called “breathing” effect[14].

MOF-based membranes have been developed and were tested for He-upgrading, but they significantly suffer from the large pore sizes, grain boundaries causing insufficient molecular sieving capabilities. Approaches have been made to combine ZIF-8 (Zeolitic Imidazolate Framework 8) and fullerenes, with one of the best results for He-upgrading so far, reaching a selectivity $\alpha(He/CH_4)$ = 9.2 with a permeance of 210 GPU at only 3.5 wt.% loading of C_{70}.[15] Thus far, MOF materials could not show to be better than existing carbon membranes.[16] Using MOFs in polymers for He-upgrading, such as HKUST-1 (Cu_3BTC_2 with BTC^{3-} =1,3,5-Benzenetricarboxylate) in Matrimid ® (a polyimide), has shown highly promising results.[17] Loading Matrimide ® membranes with 40 wt.% HKUST offered a selectivity of $\alpha(He/CH_4)$ = 392 with a He-permeability of P = 64.3 Barrer[18], but also these membranes performed

only slightly better than the benchmark from polymers, gathered by Robeson[19]. Many different synthetical approaches have been made to eliminate lattice defects and improve molecular selectivity.[20] Nevertheless, the intrinsic flexibility of MOFs has always been a key issue, and hence much research was invested to improve the porosity and tune the adsorptive features of MOFs in polymer-filler MMMs.[21] The polymer-filler combination is a crucial factor that must be taken into account during the design of the MMMs. [22]

We believe to have identified metal-organic frameworks as suitable molecular sieves starting from our recent study on gas diffusion in ZIF-62 glasses, which lost a considerable amount of its porosity upon melting and thereby became impenetrable for larger gases.[23] However, tiny gas species were still able to diffuse rapidly through these MOF-glasses, offering very precise molecular sieving.[24] This lead to the idea to revisit MOFs as molecular sieves which were until now considered as "dense" or "non-porous". The crystalline metal-organic framework MIL-116 (Matériaux de l'Institut Lavoisier 116) is among the materials considered as dense and non-porous, and seems based on its crystallographic features (i.e. void volume of the structure) suitable for He-sieving.[25,26] The term "non-porous" originates from the disability of these MOFs to take up N_2 (d_{kin} = 3.6 Å) or Ar (d_{kin} = 3.43 Å) gas, which also was the common opinion on ZIF-62[27] (and is the current opinion on MIL-116[25]). In MIL-116, non-removable crystal water is contained in the pore space, rendering the pores extremely narrow and thereby highly suitable for precise molecular sieving of He from CH_4.[25] To optimize polymer-filler interaction, we follow another concept for MMMs synthesis, which is the marriage of MOFs with polymers of the same diffusivity.[28] The solution-diffusion model as the underlying transport mechanism in polymers is highly depending on the ordering and eventual crystallinity of the polymeric chains. To reduce the impact of adsorption in the MOF-filler and the diffusion barrier, the diffusive transport through the MOF must also be slow.[28–30] When a polymer has a high density and shows very slow permeability, the MOF should also provide narrow pores and slow diffusion, while still able to enhance gas permeability of the matrix. In this study we decided for the thermoplastic high-performance polymer polysulfone (PSU), which has a very low permeability, and married it with MIL-116(Ga). Prior studies have reported significant performance for He/CH_4 and H_2/CH_4 separation with MMMs using highly fluorinated polymers[19]. Nevertheless, due to rising awareness of the toxicity and longevity of per- and polyfluorinated substances (PFAS)in the environment,[31] which comes mainly from polymer chemistry, the use of simple polymers is very favourable and investigated in this study for its feasibility.

Results and Discussion

Modulated Synthesis for Growth of Druse-Type MOF Crystals

Modulated synthesis is a concept that can be used to control the crystalline dimensions of a metal-organic framework. It is based on the addition of acids and bases to the reaction mixture, which affect the protonation of the linker molecules, thus giving control over the nucleation of the MOF. Furthermore, monocarboxylic acids (i.e. formic acid, acetic acid, benzoic acid) can be used in the synthesis of carboxylate-based MOFs, where they act as coordination modulators.[32]

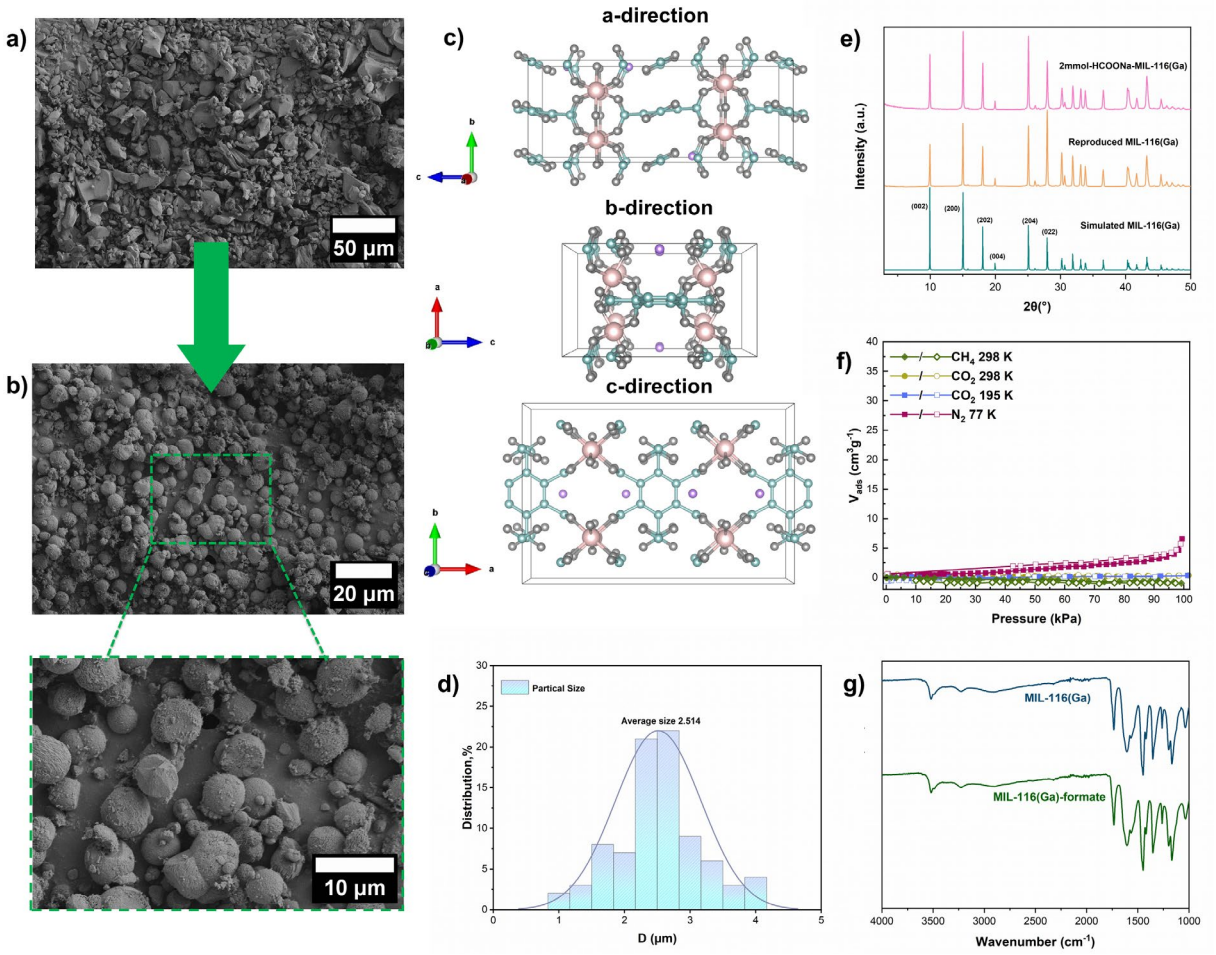

Figure 1 a) SEM image of the reproduced synthesis of MIL-116(Ga) from literature[25]. **b)** SEM images in different magnification of MIL-116(Ga) prepared by HCOONa modulated synthesis yielding monodisperse, spherical 1-5 µm (average 2.51 µm) sized particles, suitable for mixed matrix membranes preparation. **c)** The crystal structure of MIL-116(Ga) viewed along the a, b and c direction with Ga = rosé, O = grey, C = green, and H_2O = Purple. In b- and c-direction, the MOF shows channels suitable for diffusional gas transport. The pore is partly blocked by H_2O molecules that are strongly bond. The outer surface shows dangling -COOH groups, optimizing distribution in the polymer. **d)** Particle size distribution of MIL-116(Ga)-formate. **e)** XRD patterns of simulated MIL-116(Ga),, reproduced MIL-116(Ga), and modulated MIL-116(Ga)-formate. **f)** Gas sorption isotherms of MIL-116(Ga)-formate showing no micropore adsorption for CH_4, CO_2 and N_2. (**g)** IR spectra of MIL-116(Ga) and MIL-116(Ga)-formate showing no residual guest molecules of formate.

Benzoic acid for instance, works as a competitor over coordination centres for -COOH groups[33], and its use usually results in improved crystallinity and large MOF crystals.[34] Furthermore, modulators can

block certain lattice planes leading to facetted crystalline growth and thus to particle shape variations.[35] We investigated the influence of different modulators on the synthesis of MIL-116(Ga) (see **Figures S1-S5**).

The best outcome for MMM incorporation was obtained using sodium formate. SEM micrographs of the material reproduced from literature is shown in **Figure 1a**, and the micrographs of the synthesis modulated by 2 mmol/L sodium formate is shown in **Figure 1b**, offering spherical shape. MIL-116(Ga) consists of 1,2,3,4,5,6-benzenehexacarboxylic acid (mellitic acid) which is coordinated to Ga^{3+}-ions with the formula $Ga_2(OH)_2[C_{12}O_{12}H_2]\cdot 2H_2O$. In the structure the Ga^{3+}-ions are bridged by hydroxy groups, forming a 1D chain similar to the one found in the prototypical MOF MIL-53.[36] Each mellitic acid is coordinating to four individual $Ga(OH)_2$ chains with the carboxylate groups in 1, 2, 4 and 5 positions building up the network, while the two carboxylates in 3 and 6 position remain protonated and point into the pore space. The two O atoms in the carboxylates connected to the Ga ions are coordinating to neighbouring Ga within the same chain. Each Ga is surrounded by six O atoms from carboxylates and hydroxides, leading to an octahedral coordination environment The space group of MIL-116(Ga) is *CmCm*, an orthorhombic lattice forming parallelepiped-shaped crystals. Its structure in a, b, and c direction is shown in **Figure 1c**. The size distribution, counted from SEM images, is given in **Figure 1d**. The particles synthesized following sodium-formate modulations have an average size of 2.51 ± 0.65 µm.

The powder x-ray diffraction (PXRD) patterns of the crystals in **Figure 1e** show the reproduced synthesis, simulated pattern and pattern of the modulated synthesis of MIL-116(Ga). The modulated pattern shows all high intensity reflections also found in the simulated pattern from the single crystal structure and the reproduced synthesis; however, we find intensity changes for the (002), (202), (204) and (022) reflections, which is attributed to the spherical particle shape after modulation.

The pore channels through the material are visible, with no-removable H_2O molecules blocking the entrance of the pore (c.f. **Figure 1c**). Even after *in vacuo* activation at elevated temperatures, the H_2O cannot be removed from the crystal structure, rendering the pore channels non-accessible for large molecules like N_2, CO_2 and CH_4 which was confirmed through sorption experiments (see **Figure 1f** and **Figure S 6)**. The linker, even though it is a hexa-dentate linker, only coordinates with four -COOH groups, meaning that on the crystals outer surface free -COOH groups are available, offering the possibility to form H-bonds.

Thermogravimetric and differential scanning analysis (TGA and DSC) shows a small weight loss at around 100 °C, attributed to surface bond molecules, while the crystal water leaves the MOF from around 300 °C, followed by decomposition from 400 °C onward (see **Figure S7**). This means that activation of the crystal happens already at 100 °C, but crystal water remains until decomposition. From TGA and DSC we find that the sample is free of the modulator, and also the XRD shows no additional

reflections, giving a phase-pure MIL-116(Ga) pattern. Furthermore, via IR spectroscopy in **Figure 1g**, guest free spectra are obtained, comparable to the reproduced, unmodulated MIL-116(Ga).

Microstructural Investigations of the Mixed Matrix Membranes

MMMs were fabricated by doctor blading of DMF-based solutions of polysulfone (PSU) and MIL-116(Ga)-formate, giving the corresponding MMMs with 5, 10, 15, and 20 wt.% loading as well as a pure polysulfone membrane was prepared. The films are casted onto a soda-lime glass slide using a micrometre adjustable knife and are then dried in a vacuum furnace at 120 °C.

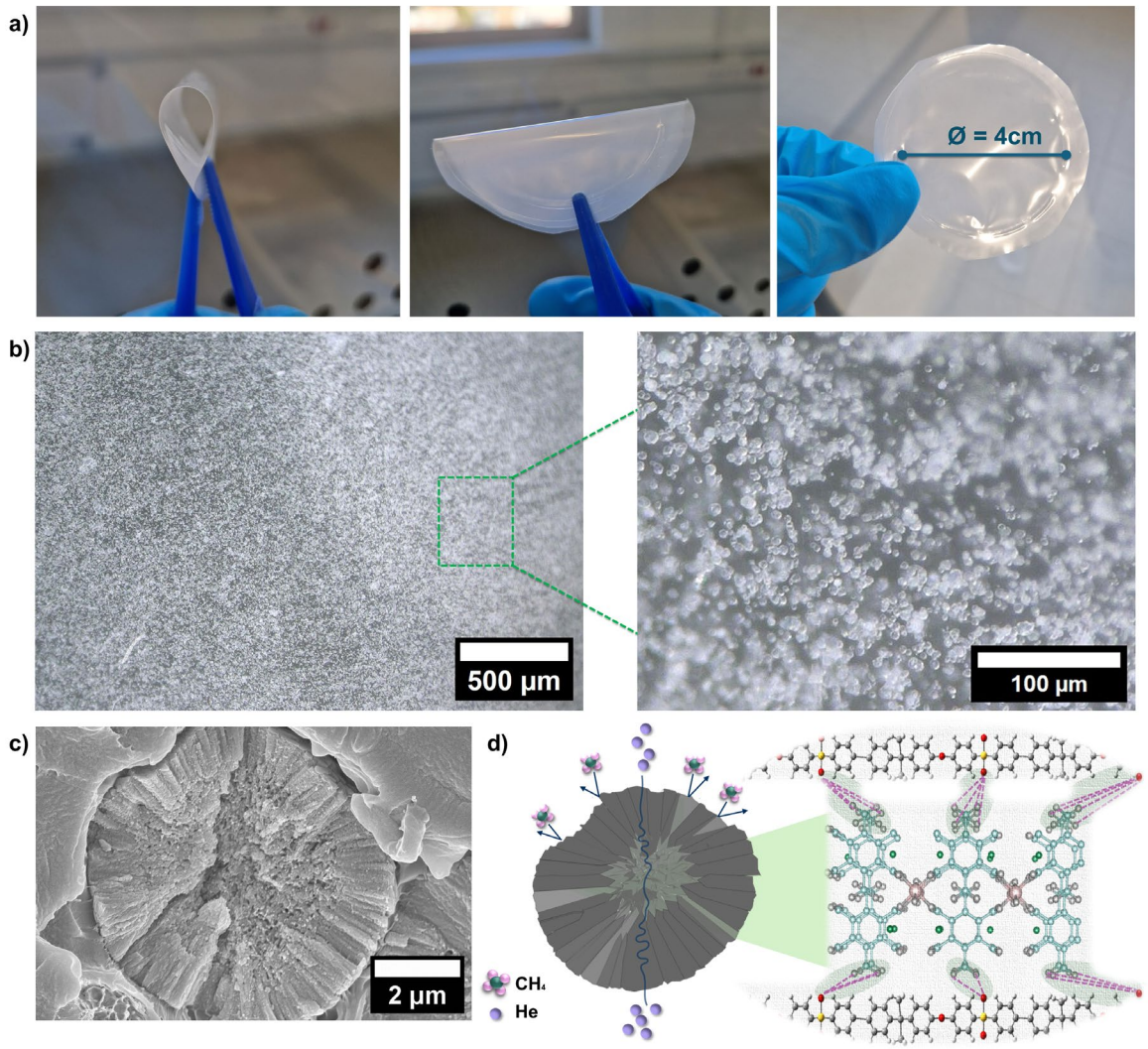

Figure 2 a) Photographs of the 5 cm diameter membrane with 20 wt.% MIL-116(Ga)-formate loading and demonstration of the remaining flexibility, after gas permeation measurement at 60 °C. **b)** Optical top-view micrographs of the 10 wt.% MIL-116(Ga)-formate PSU MMM shows homogeneous filler distribution over a large area, and the zoomed in area shows that there is no agglomeration. The particles are freely "floating" in the polymer and the polymer is highly transparent after casting. **c)** SEM image of a druse-like particle that has been cracked-open during SEM preparation of the MMM (breaking the MMM after freezing with liquid N_2). The particle shows nanoscopic lose particulate in the middle, while densified crystalline needles form a hollow-shell particle. **d)** A schematic of the hollow-sphere druse-like particle, separating CH_4 from He. It further shows the surface of MIL-116(Ga) with the dangling -COOH groups forming H-bridges to the sulfone groups of PSU[37], offering important polymer-filler interaction.

Adjusting the knife to 300 µm results in a 60-80 µm thick polymeric film after solvent removal. After casting the polymer and removing the solvent, the film appears transparent, confirming that a defect free layer was achieved The resulting film is highly homogeneous and is cut out to the desired diameter for the membrane film, as shown on photographs of the 20 wt.% MIL-116(Ga)-formate MMM in **Figure 2a**. The optical micrographs shown in **Figure 2b** is taken from the 10 wt.% MIL-116(Ga)-formate PSU MMM, which offered the best visibility of the homogeneous filler loadings. There are no large agglomerates or defect sites visible. When zoomed in, the membrane shows highly homogeneous filler distribution throughout the membrane. All MIL-116(Ga)-formate particles are well separated from another and no agglomerates form.

To perform SEM analysis of the MMMs to investigate the microstructure of the membranes further, the membranes were dipped into liquid N_2 at -196 °C for 60 seconds to break smooth cross-sections. Through this procedure we made an interesting discovery about the particle morphology, which is shown for an PSU-embedded, broken particle in **Figure 2c**.

The microstructure of the modulated MIL-116(Ga) is not a solid sphere, but a hollow-sphere from a druse-like crystal assembly. Apparently, during our synthesis these hollow spheres must form from a loose particulate, which later grows into a polycrystalline shell, consisting of individual needle like crystallites. We think that shell-induced Ostwald ripening leads to dissolution of the nanoparticles for the sake of the micron-sized shell, leading to the druse-like morphology as shown in **Figure 2c**.[38] These druse-like crystals offer interesting features for MMMs, as shown in the schematic in **Figure 2d**. For He, diffusion is enhanced in the middle of the particle, offering a highway for gas diffusion, as the average pathway over the particle is decreased. The outer surface of the MIL-116(Ga) particle is assumed to offer H-bonding to PSU.

The microstructural investigation of the PSU-based MMMs with 10, 15 and 20 wt.% MIL-116(Ga)-formate via scanning electron microscopy (SEM) is shown in **Figure 3a**, **b** and **c**. It is clearly visible that the particles, despite their size of ~2.5 µm do not show any sign of sedimentation. Instead, a good distribution and defect-free MMMs with thicknesses of 63 µm and 72 µm with and increasing filler content are observed.

In **Figure 3d** an SEM analysis and energy dispersive X-ray spectroscopy (EDX), including EDX mapping (EDXM) of an MMM with 20 wt.% is shown. EDXM of MMMs with 10 wt.% and 15 wt.% are shown in the **Figures S8-S9**. The mixed map in **Figure 3d** gives insights on the distribution of the filler in the MMMs.

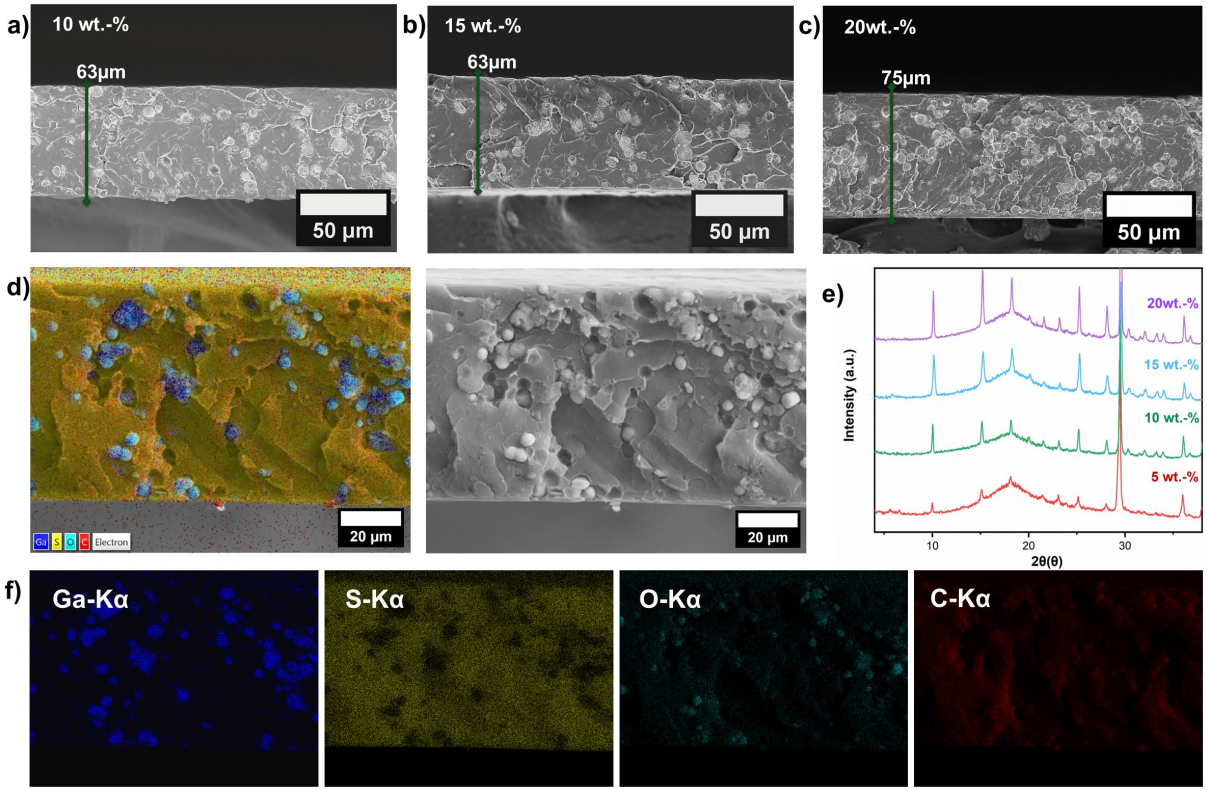

Figure 3 a) Cross-sectional SEM image of the PSU MMM with 10 wt.-% MIL-116(Ga)-formate. **b)** SEM image of the PSU MMM with 15 wt.% MIL-116(Ga)-formate. **c)** SEM image of the PSU MMM with the cross section of 20 wt.% MIL-116(Ga)-formate. **d)** EDX analysis mixed elemental map of the 20 wt.% sample showing position of MOF particles and polymer in the membrane. S = yellow, Ga = blue, O = turquoise, C = red. **e)** Shows the PXRDs of the MOF inside the polymer. The intensity of the MOF x-ray reflections increases with higher filler content. The relatively strong diffraction peak at $2\theta = 29°$ originates from the sample holder and represents the Si (111) diffraction peak. **f)** Shows the single element maps from d), with S = yellow, Ga = blue, O = turquoise, C = red. Signals of O and C are found in the MOF and the polymer, while Ga is only found in the MOF and S only in the Polymer.

The filler itself does not lose crystallinity upon polymer incorporation and activation of the MMM, and the powder diffraction patterns recorded for the MMMs show increased diffraction intensity for higher wt.% MOF loading in **Figure 3e**. The (111) reflex at ~29 °2θ of the Si sample holder is visible, which was used for heights error correction. The single elemental maps from the EDX mapping (**Figure 3f**) demonstrate the elemental distribution in different areas of the MMM. It is clearly visible that PSU shows a high signal for S-Kα and C-Kα, and low contents of O-Kα x-rays, while the MIL-116(Ga)-formate filler shows high signals for Ga-Kα and O-Kα, and smaller signal for C-Kα x-rays.

Gas Permeation for the Separation of He/CH_4

To evaluate the membrane performance via gas permeation we decided to immediately measure binary gas mixture of He and CH_4. A home-built Wicke-Kallenbach membrane permeator is used, which is operated at 60 °C and without feed pressure. Before the experiment, the membranes were activated in a vacuum oven and the membranes were routinely checked for their pressure resistance in the device before measurement. We simulate a mixture of He in a natural gas (CH_4) reservoir of 4 %, mimicking the real-world process from a feedstock. In the upstream, the feed gas was adjusted to be 100 ml/min,

meaning 4 ml/min He and 96 ml/min CH_4, controlled by mass flow controllers, while N_2 was used as a sweep gas on the downstream with 1 ml/min, carrying the permeate to the gas chromatograph. This allows for a continuous measurement at equilibrium conditions.

The results are shown in **Figure 4a**. We measured the neat PSU first, leading to comparable results as reported earlier.[39] As expected, the small gas He has a high permeability through the PSU, while CH_4 is diffusion limited already by the polymer. Incorporated MIL-116(Ga) filler with 5, 10, 15 and 20 wt.% is compared in its performance, showing a clear trend. The He permeability is increased with increasing filler content, while the permeability of CH_4 is decreasing with increasing filler content, giving a trend to high selectivity with higher loading.

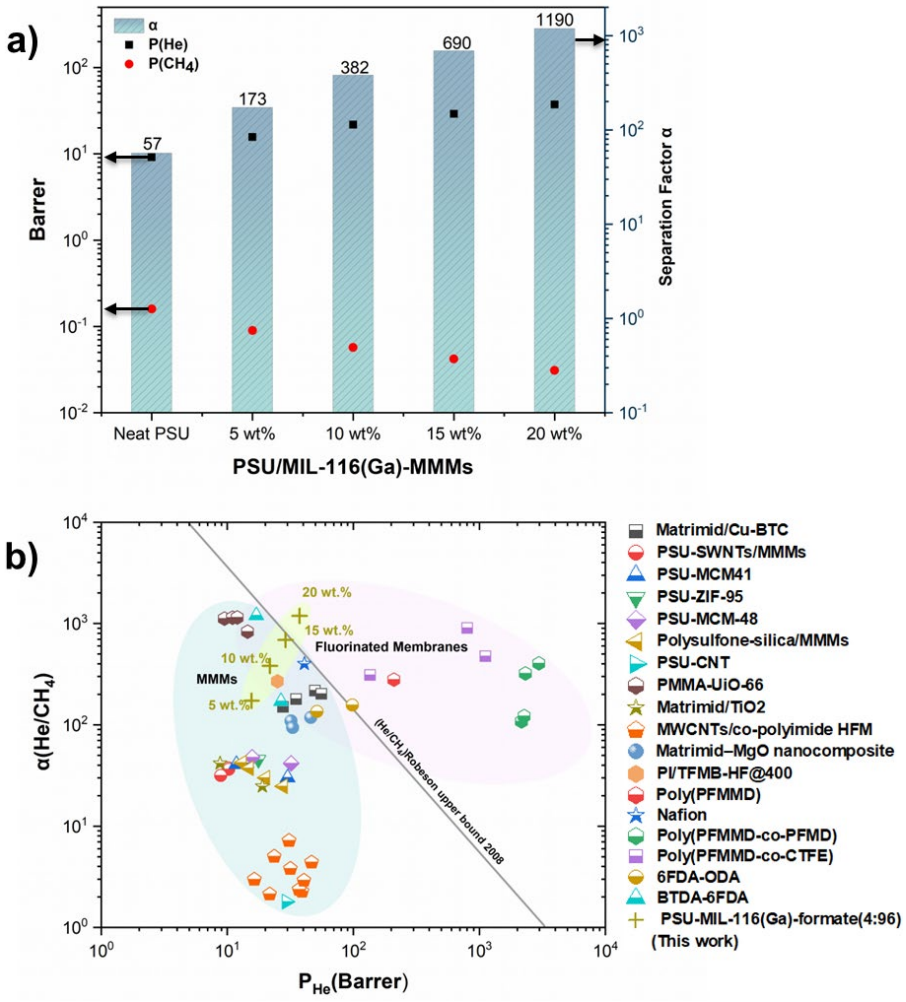

Figure 4 a) Permeability P in Barrer (left Y-axis, points) and separation factor α (right Y-axis, bars) of the PSU MMMs against the MOF-loading of 0 (neat polymer), 5, 10, 15 and 20 wt.% MIL-116(Ga)-formate. **b)** Benchmarking of the MIL-116(Ga)-formate MMMs against other materials employed in He/CH_4 separation, including the Robeson Upper Bound (2008) for He/CH_4. It must be noted that our data has been collected for a 4:96 He/CH_4 mixed feed gas following process conditions, while all other data referenced comes from 50:50 mixtures.[25,29,39,40] Some literature gas permeation data sets were conducted through constant-volume/variable-pressure apparatus, rendering direct comparison challenging. The comparison table can be found in the **Table S3**.

While the neat PSU offers a permeability of P(He) = 9.13 Barrer and P(CH_4) = 0.16 Barrer with a selectivity α(He/CH_4) = 57, following an almost linear trend the 20wt.% MIL-116(Ga) MMM offers a permeability P(He) = 37.40 Barrer and P(CH_4) = 0.03 Barrer and a selectivity of α(He/CH_4) = 1190. It must be stressed that these values have been generated for a feed mixture of 4:96 He to CH_4, offering a huge increase in performance when considering the differences in chemical potential to a 50:50 mixture. The fact that CH_4 permeability declines and He permeability increases with increasing MIL-116(Ga) content means that the MMMs operate highly diffusion selective and the concept of using "dense" MOFs has proven to be an interesting feature for high precision molecular sieving.

A comparison plot is shown in **Figure 4b** with the faster permeating species (He) on the x-axis and the selectivity on the y-axis in a so-called Robeson-plot. Comparing our MMMs to MMMs containing other materials as fillers, such as CNTs (Carbon Nanotubes), MCM-41 (Mobil Composition of Matter No. 41), ZIFs and other nanocomposites, as well as to the polymeric membrane benchmark (Robeson upper bound) it is clearly visible that the MIL-116(Ga)-formate MMMs with 15 and 20 wt.% surpass the other materials by far. We also compare our MMMs with fluorinated membranes such as Nafion™, PFMMD (perfluoro(2-methylene-4-methyl-1,3-dioxolane) and our 15 and 20 wt.% MMMs entering in region of fluorinated membranes without having hazardous impact on both environment and humans during and after their production, eliminating effects of fluorinated forever-chemicals[41].

Considering that our membranes are measured with a mixture of 4% He and 96% CH_4, with a much lower chemical potential for He diffusion than for 50:50 mixtures, also the 5 and 10 wt.% membranes probably surpass the other comparable materials. However, a comparison is challenging as the body of research in the literature is still comparably small and measurement protocols differ vastly in literature. Measurement parameters and exact numbers can be found in the **Table S3**. Nevertheless, it is worth mentioning that our membranes offer a performance much higher than comparable materials and surpasses the Robeson upper bound 2008, which is also only comparing data for 1:1 mixture of He and CH_4. With the MIL-116(Ga-formate) MMMs with 20 wt.% we can upgrade He from 4 % to a purity of 99.997% (technical grade of He 4.6) directly from a natural gas stream in a one-step process.

Conclusion

This study provides a straightforward approach towards highly diffusion-selective mixed matrix membranes (MMMs) to upgrade He from CH_4. In summary, we have developed a modulated synthesized approach, yielding druse-type hollow crystals of MIL-116(Ga), a so called "dense" metal organic framework (MOF). MIL-116(Ga) is non-porous towards gases such as CO_2 and N_2 due to crystal water in its structure, as shown in its crystal structure and in sorption measurements. However, it offers the possibility for diffusive permeation of He with the kinetic diameter d_{kin} = 2.6 Å. The free pathway inside the crystal druse allows to speed up diffusion, while completely reflecting CH_4 at its surface, making MIL-116(Ga)-formate an ideal molecular sieve. Through incorporation of the druse-like MIL-

116(Ga)-formate crystals into a polysulfone (PSU) matrix, an inexpensive and diffusion limiting polymer, high performance MMMs were made. From microstructural investigations, an ideal polymer-filler interaction is observed, attributed to H-bonding between -COOH groups of the MOF and PSU. The MMMs were loaded with MIL-116(Ga)-formate in 5, 10, 15 and 20 wt.% and their performance for He/CH_4 separation was measured mimicking process conditions with 4 % He in the binary gas mixture. The MIL-116(Ga)-formate filler strongly increases the permeability of He, while at the same time strongly decreasing the permeability for CH_4. The 20 wt.% MIL-116(Ga)-formate MMM exceeds comparable composites and polymers and breaks the Robeson benchmark by far, with He permeability P(He) = 37,40 Barrer and $\alpha(He/CH_4)$ = 1190. With such a MMM we can reach regions for He/CH_4 separation, thus far only reachable with expensive fluorinated polymers. This reduced the environmental impact and is cost efficient. With this membrane it is possible to upgrade 4 % He in 96 % Methane to 99.997 % pure He, technical grade He 4.6 as sold in the markets.

Experimental Section:

Modulated Synthesis of MIL-116(Ga)

The reference material was prepared following the original literature by Volkringer et al.[25,29], which synthesis was then varied to achieve a different particle shape. The optimized modulated MIL-116(Ga) synthesis protocol is as follows: $Ga(NO_3)_3\,xH_2O$ (2.4 g, 9.4 mmol) was dissolved in 20 mL of de-ionized water (DI water) and stirred. Then, mellitic acid (1.198 g, 3.50 mmol) was added and stirred until fully dissolved. Sodium formate (0.81612 g, 12 mmol) was dissolved in 10 mL of DI water. The two solutions were mixed, stirred for another 5-10 minutes and transferred to a Teflon-lined autoclave. The autoclave was sealed and heated at 210 °C for 24 hours in a furnace. White crystalline particles were collected by centrifugation at 9000 rpm for 10 minutes, washed thrice with DI water and dried at 40 °C for 24 hours. The same procedure was followed using different amounts of HCOONa (see **Figure S1**). Different modulators were tried to manipulate the particle morphology of MIL-116(Ga). For more experimental details, please refer to **Table S1-S2** in the supporting Information.

Synthesis of PSU-MIL-116(Ga) Mixed Matrix Membranes (MMMs)

For MMMs synthesis, the neat PSU and four different loadings (5, 10, 15 and 20 wt.%) of MIL-116 (Ga)-formate were prepared by dissolving the corresponding amount of filler in the solution of PSU with a reference mass of 1 g total in 3 ml of DMF and stirred for 24 hours to get a homogenous solution. The resulting solution was cast using a doctor blade (BYK, Germany) on a clean glass plate with an automatic film applicator. To ensure uniform formation of a film during curing, the glass substrate was covered with a glass cover to slow down the evaporation process. The Glass plate was then placed into the oven for curing at 110 °C overnight. Thickness measurements for the prepared membranes were performed via SEM. The thickness of the measured films was around 60 µm to 80 µm (see SEM images).

Gas Permeation Experiments

Membrane performances were evaluated in a custom-built Wicke Kallenbach gas permeation setup. The prepared MIL-116 (Ga)-formate PSU membranes were placed in a stainless-steel membrane module (offering an effective membrane area of 4.01 cm^2) and sealed gastight by Viton® O-rings to prevent leakage. For practical testing for He separation (4:96 He:CH_4 mixture), He and CH_4 were supplied at flow rates of 4 mL/min and 96 mL/min respectively at 60 °C keeping pressure at 1 bar. The permeate side was swept with N_2 at 1 ml/min. The composition of the permeate side stream was analysed by a gas chromatography system from Shimadzu (GC-2030 Nexis).

Optical Microscopy

A digital Microscope VHX-6000 by Keyence was used for microscopic images of the MIL-116 (Ga)powder and films. A universal zoom lens VH-Z100UR with a magnification range of 100x to 1000x was used. The XRD data was recorded using Rigaku MiniFlex diffractometer with a 600 W X-ray generator (Cu Kα X-ray radiation, λ = 1.54 Å). The Bragg–Brentano geometry was used in the 3.00-40.00°2θ range along the step size of 0.02 °.

FT-IR Spectroscopy

The FT-IR spectra were recorded in a VERTEX 70 (Bruker). The IR spectra were acquired using the attenuated total reflectance (ATR) mode in a range of 4000 - 600 cm^{-1}. For this, roughly 2 mg of the sample were placed on the diamond of the ATR unit. Prior to every measurement, a background spectrum was recorded and subtracted from the spectra of the material.

Scanning Electron Microscopy and Energy Dispersive X-Ray Spectroscopy

An Oxford EDX system in combination with a Sigma VP Field Emission Scanning Electron Microscope was used to analyse the samples. For cross-section samples the membranes were fractured in liquid nitrogen to preserve their microstructures. Afterwards, the samples were fixed to carbon adhesive discs and a small amount of conductive silver paint was added to ensure good conductivity. Finally, the samples were coated with Pt (5 nm) in a high vacuum sputter coater (Safematic CCU-O10 HV) to avoid charging effects. The SEM micrographs were obtained from a Sigma VP field Emission Scanning Electron Microscope (Carl-Zeiss AG, Germany). SEM micrographs were performed with an acceleration voltage of 6 - 8 kV an emission current of 271 - 289 pA and using SE2 and InLens detectors. EDX samples were prepared as mentioned above but using a coating of Pt (8 nm). EDS investigations were performed with an Oxford system and a 50 mm^2 XMax detector with a resolution of 127 eV. Mapping was performed during 20-30 minutes with an acceleration voltage of 20 kV.

Acknowledgements

A. Ko, L.C.R., O.S., T.H., R.W., F.H.S. and A. K. acknowledge support by the Free State of Thuringia and the European Social Fund Plus within the 2022 FGR 0039 and 0040. A.K. thanks the German Science Foundation (DFG) for support within the priority program SPP 1928/2 COORNETs under grant

number 434440165. A.K. further thanks the Carl Zeiss Foundation for funding within the "Breakthroughs" program. The SEM facilities of the Jena Center for Soft Matter (JCSM) were established with a grant from the German Research Council (DFG). A. S. Gratefully acknowledges the Fonds der Chemischen Industrie for a Liebig Fellowship.

Conflict of Interest

The authors declare no conflict of interest.

Data Availability Statement

The data that support the findings of this study are available in the supplementary material of this article.

References

[1] a) F. Scheller, S. Wald, H. Kondziella, P. A. Gunkel, T. Bruckner, D. Keles, *Sustain. Energy Technol. Assess.* **2023**, *56*, 103037; b) J. Rosen, *Science* **2023**, *382*, 624.
[2] B. Birner, J. Severinghaus, B. Paplawsky, R. F. Keeling, *Nat. Geosci.* **2022**, *15*, 346.
[3] D. Kramer, *Phys. Today* **2023**, *76*, 18.
[4] C. J. Berganza, J. H. Zhang, *Med. Gas Res.* **2013**, *3*, 18.
[5] M. Ramli, K. Kagawa, S. N. Abdulmadjid, N. Idris, W. S. Budi, M. A. Marpaung, K. H. Kurniawan, T. J. Lie, M. M. Suliyanti, R. Hedwig et al., *Appl. Phys. B* **2007**, *86*, 729.
[6] S. T. Anderson, *Nat. Resour. Res.* **2018**, *27*, 455.
[7] A. A. Kiss, R. Smith, *Energy* **2020**, *203*, 117788.
[8] O. Smirnova, S. Ojha, A. De, A. Schneemann, F. Haase, A. Knebel, *Adv. Funct. Mater.* **2023**.
[9] a) W. Zhou, H. Wu, M. R. Hartman, T. Yildirim, *J. Phys. Chem. C* **2007**, *111*, 16131; b) J. A. Villajos, R. Balderas-Xicohténcatl, A. N. Al Shakhs, Á. Berenguer-Murcia, C. E. Buckley, D. Cazorla-Amorós, G. Charalambopoulou, F. Couturas, F. Cuevas, D. Fairen-Jimenez et al., *ChemPhysChem.* **2024**, e202300794.
[10] A. Knebel, J. Caro, *Nat. Nanotechnol.* **2022**, *17*, 911.
[11] a) S. Horike, S. Shimomura, S. Kitagawa, *Nat. Chem.* **2009**, *1*, 695; b) H. Jiang, S. Benzaria, N. Alsadun, J. Jia, J. Czaban-Jóźwiak, V. Guillerm, A. Shkurenko, Z. Thiam, M. Bonneau, V. K. Maka et al., *Science* **2024**, *386*, 659.
[12] A. Knebel, B. Geppert, K. Volgmann, D. I. Kolokolov, A. G. Stepanov, J. Twiefel, P. Heitjans, D. Volkmer, J. Caro, *Science* **2017**, *358*, 347.
[13] M. R. Ryder, B. Civalleri, G. Cinque, J.-C. Tan, *CrystEngComm* **2016**, *18*, 4303.
[14] S. Hyun, J. H. Lee, G. Y. Jung, Y. K. Kim, T. K. Kim, S. Jeoung, S. K. Kwak, D. Moon, H. R. Moon, *Inorg. Chem.* **2016**, *55*, 1920.
[15] J. Han, H. Wu, H. Fan, L. Ding, G. Hai, J. Caro, H. Wang, *J. Am. Chem. Soc.* **2023**, *145*, 14793.
[16] Q. Wu, L. Liu, Y. Jiao, Z. Li, J. Bai, X. Ma, S. Luo, S. Zhang, *Angew. Chem. Int. Ed.* **2024**, *63*, e202400688.
[17] a) A. Akbari, J. Karimi-Sabet, S. M. Ghoreishi, *Chem. Eng. Process.* **2020**, *148*, 107804; b) M. M. Khan, V. Filiz, G. Bengtson, S. Shishatskiy, M. M. Rahman, J. Lillepaerg, V. Abetz, *J. Mem. Sci.* **2013**, *436*, 109.
[18] Z. Wang, D. Wang, S. Zhang, L. Hu, J. Jin, *Adv. Mater.* **2016**, *28*, 3399.
[19] L. M. Robeson, *J. Mem. Sci.* **2008**, *320*, 390.
[20] G. Liu, Y. Guo, C. Chen, Y. Lu, G. Chen, G. Liu, Y. Han, W. Jin, N. Xu, *Nat. Mater.* **2023**, *22*, 769.
[21] E. Esposito, M. Carta, A. Fuoco, M. Monteleone, B. Comesaña-Gándara, E. Gkaniatsou, C. Sicard, S. Wang, C. Serre, N. B. McKeown et al., *J. Mem. Sci.* **2024**, *697*, 122475.
[22] a) A. Knebel, A. Bavykina, S. J. Datta, L. Sundermann, L. Garzon-Tovar, Y. Lebedev, S. Durini, R. Ahmad, S. M. Kozlov, G. Shterk et al., *Nat. Mater.* **2020**, *19*, 1346; b) T. T. Moore, W. J. Koros, *J. Mol. Struct.* **2005**, *739*, 87.
[23] T. D. Bennett, Y. Yue, P. Li, A. Qiao, H. Tao, N. G. Greaves, T. Richards, G. I. Lampronti, S. A. T. Redfern, F. Blanc et al., *J. Am. Chem. Soc.* **2016**, *138*, 3484.
[24] O. Smirnova, S. Hwang, R. Sajzew, L. Ge, A. Reupert, V. Nozari, S. Savani, C. Chmelik, M. R. Reithofer, L. Wondraczek et al., *Nat. Mater.* **2024**, *23*, 262.

[25] C. Volkringer, T. Loiseau, N. Guillou, G. Férey, D. Popov, M. Burghammer, C. Riekel, *Solid State Sci.* **2013**, *26*, 38.
[26] E. V. Alexandrov, A. V. Goltsev, R. A. Eremin, V. A. Blatov, *J. Phys. Chem. C* **2019**, *123*, 24651.
[27] R. Banerjee, A. Phan, B. Wang, C. Knobler, H. Furukawa, M. O'Keeffe, O. M. Yaghi, *Science* **2008**, *319*, 939.
[28] A. M. Thomas, J. de Grooth, J. A. Wood, *J. Mem. Sci.* **2022**, *649*, 120311.
[29] J. Ahn, W.-J. Chung, I. Pinnau, M. D. Guiver, *J. Mem. Sci.* **2008**, *314*, 123.
[30] J. Kärger, T. Binder, C. Chmelik, F. Hibbe, H. Krautscheid, R. Krishna, J. Weitkamp, *Nat. Mater.* **2014**, *13*, 333.
[31] a) J. R. Kuiper, S. H. Liu, B. P. Lanphear, A. M. Calafat, K. M. Cecil, Y. Xu, K. Yolton, H. J. Kalkwarf, A. Chen, J. M. Braun et al., *Am. J. Epidemiol.* **2024**; b) Y. Zhang, Y. Zhou, R. Dong, N. Song, M. Hong, J. Li, J. Yu, D. Kong, *J. Hazard. Mater.* **2024**, *465*, 133270.
[32] H. Guo, Y. Zhu, S. Wang, S. Su, L. Zhou, H. Zhang, *Chem. Mater.* **2012**, *24*, 444.
[33] A. Schaate, P. Roy, A. Godt, J. Lippke, F. Waltz, M. Wiebcke, P. Behrens, *Chem. Eur. J.* **2011**, *17*, 6643.
[34] M. G. Goesten, M. F. de Lange, A. I. Olivos-Suarez, A. V. Bavykina, P. Serra-Crespo, C. Krywka, F. M. Bickelhaupt, F. Kapteijn, J. Gascon, *Nat. Commun.* **2016**, *7*, 11832.
[35] J. Cravillon, C. A. Schröder, H. Bux, A. Rothkirch, J. Caro, M. Wiebcke, *CrystEngComm* **2012**, *14*, 492.
[36] C. Volkringer, T. Loiseau, N. Guillou, G. Férey, E. Elkaïm, A. Vimont, *Dalton Trans.* **2009**, 2241.
[37] B. D. Reid, F. A. Ruiz-Trevino, I. H. Musselman, K. J. Balkus, J. P. Ferraris, *Chem. Mater.* **2001**, *13*, 2366.
[38] L. Yu, R. Han, X. Sang, J. Liu, M. P. Thomas, B. M. Hudak, A. Patel, K. Page, B. S. Guiton, *ACS nano* **2018**, *12*, 9051.
[39] S. Shafiq, B. A. Al-Maythalony, M. Usman, M. S. Ba-Shammakh, A. A. Al-Shammari, *RSC Adv.* **2021**, *11*, 34319.
[40] a) A. Akbari, J. Karimi-Sabet, S. M. Ghoreishi, *Chem. Eng. Process.* **2020**, *148*, 107804; b) S. Kim, L. Chen, J. K. Johnson, E. Marand, *J. Mem. Sci.* **2007**, *294*, 147; c) S. Kim, E. Marand, *Micropor. Mesopor. Mater.* **2008**, *114*, 129; d) S. Kim, E. Marand, J. Ida, V. V. Guliants, *Chem. Mater.* **2006**, *18*, 1149; e) S. Kim, J. R. Jinschek, H. Chen, D. S. Sholl, E. Marand, *Nano Lett.* **2007**, *7*, 2806; f) H. Molavi, A. Shojaei, S. A. Mousavi, *J. Mater. Chem. A* **2018**, *6*, 2775; g) F. Moghadam, M.R. Omidkhah, E. Vasheghani-Farahani, M.Z. Pedram, F. Dorosti, *Sep. Purif. Technol.* **2011**, *77*, 128; h) S. S. Hosseini, Y. Li, T.-S. Chung, Y. Liu, *J. Mem. Sci.* **2007**, *302*, 207; i) E. P. Favvas, K. L. Stefanopoulos, J. W. Nolan, S. K. Papageorgiou, A. C. Mitropoulos, D. Lairez, *Sep. Purif. Technol.* **2014**, *132*, 336; j) C. Wang, Z. Li, J. Bai, H. Liu, X. Wang, S. Luo, *Sep. Purif. Technol.* **2025**, *354*, 129019; k) M. R. Coleman, W. J. Koros, *J. Polym. Sci. B Polym. Phys.* **1994**, *32*, 1915; l) J. S. Chiou, D. R. Paul, *Ind. Eng. Chem. Res.* **1988**, *27*, 2161; m) M. Fang, Z. He, T. C. Merkel, Y. Okamoto, *J. Mater. Chem. A* **2018**, *6*, 652; n) M. Yavari, M. Fang, H. Nguyen, T. C. Merkel, H. Lin, Y. Okamoto, *Macromol.* **2018**, *51*, 2489; o) D. R. B. Walker, W. J. Koros, *J. Mem. Sci.* **1991**, *55*, 99.
[41] S. Y. Wee, A. Z. Aris, *npj Clean Water* **2023**, *6*.